

Reverse Time Migration and Amplitude Preservation

Suhas Phadke

Computational Research Laboratories Ltd., Pune, India

Abstract

Recently prestack Reverse time migration (RTM) algorithm for depth imaging has become feasible due to advances in computational power and clever programming techniques. RTM uses full acoustic two-way wave propagation algorithm for both forward and reverse time extrapolation. Amplitude preservation is based upon the assumption that acoustic wave equation approximates the wave propagation in real elastic earth. In this paper, first the amplitude characteristics of both the acoustic and elastic wave propagation are compared by looking at the reflection coefficients for a simple flat layered model. Then the input gathers generated by both acoustic and elastic forward modeling algorithm are migrated with RTM method. The amplitude behavior of the RTM algorithm is studied by looking at the amplitudes of migrated gathers. The study shows that even for a simple flat layered earth model the assumption of acoustic wave propagation in RTM may not be valid. Therefore special care must be taken while interpreting amplitude information on migrated gathers.

Introduction

Prestack Reverse Time Migration (RTM) is a state of the art depth migration technique for imaging subsurface geological structures from the recorded seismic data (Baysal et al., 1983; McMechan, 1983; Yoon et al., 2003; Farmer et al., 2006). The strength of RTM is based upon the fact that it uses a two-way acoustic wave equation for both forward and reverse time extrapolation, thus improving imaging in areas where complex geology violates the assumptions made in Kirchhoff or one-way wave equation based migration. The affordable availability of computer power and advances in programming techniques have made it feasible to apply prestack RTM algorithm to field data sets.

One of the main concerns for any seismic imaging algorithm is the amplitude preservation. Prestack imaging technique that produces correct amplitudes is a prerequisite for any study that utilizes amplitudes, e.g. AVO analysis, AVA inversion etc. The migration algorithm must be dynamically and kinematically correct. If all the propagation related losses are corrected for, the correct wave propagation equation is used for moving the energy around and proper imaging condition is applied, only then the data can be processed in a true amplitude manner. An accurate wave propagation methodology must be used in the imaging algorithm for accurate amplitude preservation.

In this paper we first take a look at the acoustic and elastic wave propagation algorithms and study their amplitude characteristics by observing the reflection coefficients as a function of angle of incidence. We shall use only 2D wave propagation algorithms here, which can be easily extended to 3D. Next we generate the synthetic data for a simple flat reflector model using both the acoustic and elastic wave propagation algorithm. Both the synthetic data sets are then migrated by RTM algorithm. The migrated gathers are then

compared for studying the amplitude preservation characteristics of RTM.

Acoustic and Elastic Wave Propagation

In seismic data processing, wave propagation in a 2D heterogeneous medium can be described either by an acoustic wave equation or an elastic wave equation (Virieux, 1986; Yerneni, 2002). Both the equations can be written as a first order system of hyperbolic equations

$$\frac{\partial Q}{\partial t} = A \frac{\partial Q}{\partial X} + B \frac{\partial Q}{\partial Z} \quad (1)$$

Where Q, A and B for acoustic wave propagation are given by

$$Q = \begin{bmatrix} p \\ \dot{u} \\ \dot{w} \end{bmatrix}, A = \begin{bmatrix} 0 & K & 0 \\ \rho^{-1} & 0 & 0 \\ 0 & 0 & 0 \end{bmatrix} \text{ and } B = \begin{bmatrix} 0 & K & 0 \\ 0 & 0 & 0 \\ \rho^{-1} & 0 & 0 \end{bmatrix}$$

and Q, A and B for elastic wave propagation are given by

$$Q = \begin{bmatrix} \dot{u} \\ \dot{w} \\ \sigma_{xx} \\ \sigma_{yy} \\ \sigma_{zz} \end{bmatrix}, A = \begin{bmatrix} 0 & 0 & \rho^{-1} & 0 & 0 \\ 0 & 0 & 0 & 0 & \rho^{-1} \\ \lambda+2\mu & 0 & 0 & 0 & 0 \\ \lambda & 0 & 0 & 0 & 0 \\ 0 & \mu & 0 & 0 & 0 \end{bmatrix}$$

$$\text{and } B = \begin{bmatrix} 0 & 0 & 0 & 0 & \rho^{-1} \\ 0 & 0 & 0 & \rho^{-1} & 0 \\ 0 & \lambda & 0 & 0 & 0 \\ 0 & \lambda+2\mu & 0 & 0 & 0 \\ \mu & 0 & 0 & 0 & 0 \end{bmatrix}$$

where p is pressure, u & w are particle velocities in x and z directions, σ_{xx} , σ_{yy} & σ_{zz} are the stress components, K is incompressibility, λ and μ are Lamé parameters and ρ is density. Model is discretized by dividing it into a number of rectangular cells and replacing each cell by a grid point. Equation (1) is solved by applying a finite difference (FD) scheme. In both, the forward propagation and reverse time extrapolation, a MacCormack type scheme is used in this paper. The FD scheme is implemented on a multiprocessor platform (Supercomputing system EKA) by using a domain decomposition scheme.

Reflection Coefficients

In order to study reflection coefficients we consider two models. Reflection coefficients for these models are calculated by using Zoeppritz's equation (Aki and Richards, 1980) which is derived from the plane wave solution of the wave equation. A simple two layer model is shown in Figure 1, which represents a marine type of model. The upper layer is the water layer underlain by an elastic layer. The physical parameters of the two layers are as shown in the figure. First we ignore the elasticity of the lower layer and generate the reflection coefficients. Next we generate the reflection coefficients by considering the lower layer to be elastic. Figure 2 shows the reflection coefficients as a function of angle of incidence for both the cases. The blue line in Figure 2 illustrates the reflection coefficient when both the layers are assumed acoustic and the red line shows the reflection coefficient for acoustic/elastic interface. One can easily observe the difference in the reflection coefficients. The reflection coefficient for acoustic/acoustic interface increases monotonically till critical angle as a function of incidence angle, whereas the

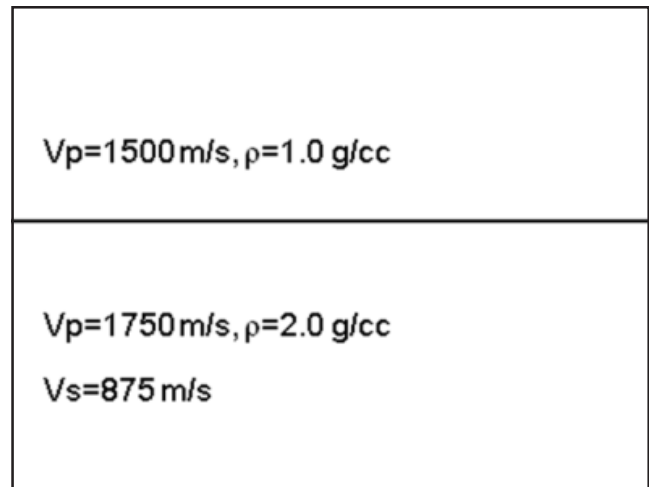


Fig. 1 A simple two layer model for studying the reflection coefficients for acoustic /acoustic and acoustic/elastic interface.

reflection coefficient for acoustic/elastic interface first decreases and then increases.

The second model is a gas sand model where a layer of gas sand is sandwiched between two shale layers. Figure 3 shows the physical parameters of the model. Figure 4 illustrates the reflection coefficients for the shale/sand interface i.e. upper interface. As expected the reflection coefficient is negative as we go from high velocity medium to low velocity medium. Again we see a difference between the acoustic assumption and elastic assumption. Figure 5 shows the reflection coefficient for the lower interface i.e. sand/shale interface. Here the reflection coefficients for acoustic assumption and elastic assumption increase till the critical angle, but their magnitudes differ.

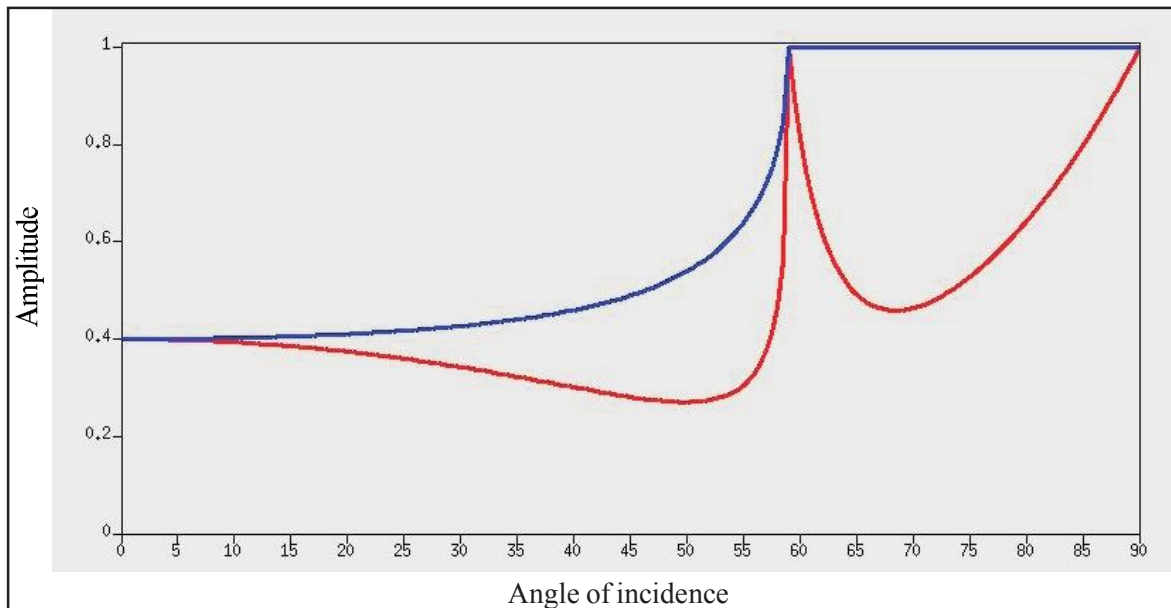


Fig.2 Reflection coefficient as a function of angle of incidence for the model shown in Figure 1. Blue line is for acoustic/ acoustic interface and the red line is for acoustic/elastic interface.

$V_p=2250 \text{ m/s}, V_s=1125 \text{ m/s}, \rho=2.0 \text{ g/cc}$
$V_p=2000 \text{ m/s}, V_s=1310 \text{ m/s}, \rho=1.95 \text{ g/cc}$
$V_p=2250 \text{ m/s}, V_s=1125 \text{ m/s}, \rho=2.0 \text{ g/cc}$

Fig.3 A gas sand model. The gas sand layer is sandwiched between two shale layers.

From these observations we infer that by assuming the medium to be acoustic and carrying out wave propagation using acoustic wave equation, we are not correctly modeling the reflection coefficients. Therefore any algorithm based upon acoustic wave equation will not be able to correctly carry out amplitude preservation.

RTM makes use of the solution of equation (1) in the following manner. The algorithm is implemented in shot gather domain. First the forward extrapolation of the source wavefield is carried out for each shot location through the gridded velocity model using finite difference method. The wavefield must be stored at each time step for application of imaging condition. Next the recorded wavefield (shot gathers)

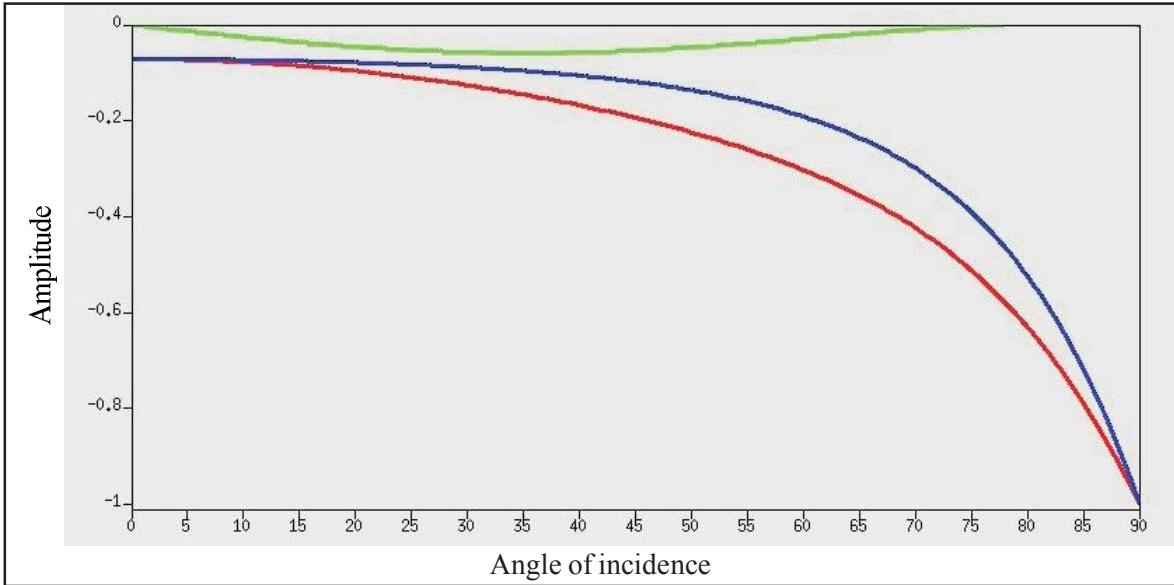


Fig.4 Reflection coefficient as a function of angle of incidence for the shale/sand interface of the model shown in Figure 3. Blue line is for acoustic/acoustic interface, the red line is for elastic/elastic interface and the green line is for converted wave with elastic/elastic interface.

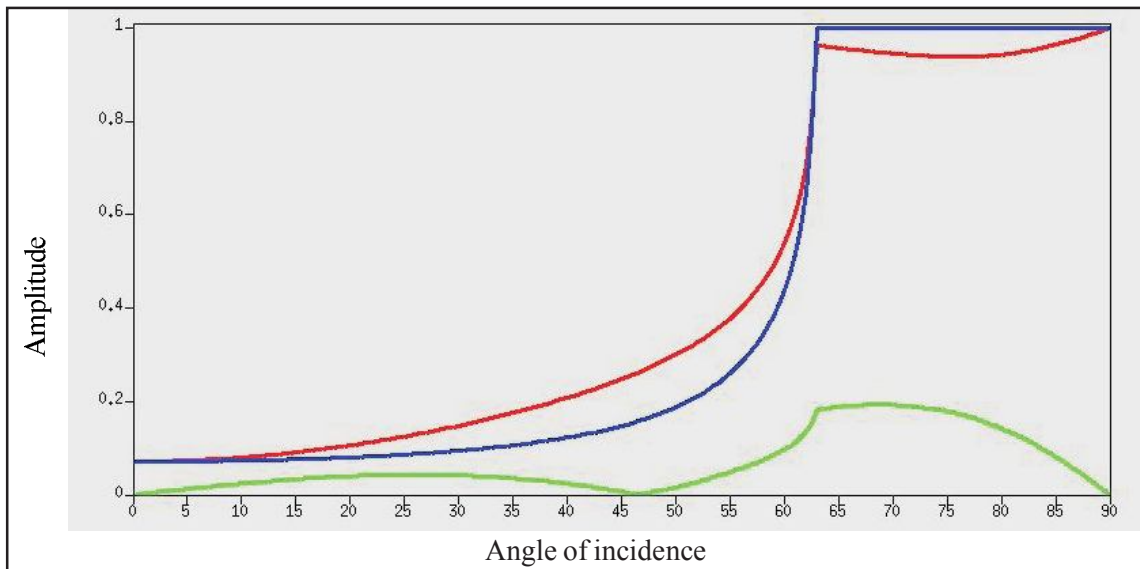


Fig.5 Reflection coefficient as a function of angle of incidence for the sand/shale interface of the model shown in Figure 3. Blue line is for acoustic/acoustic interface, the red line is for elastic/elastic interface and the green line is for converted wave with elastic/elastic interface.

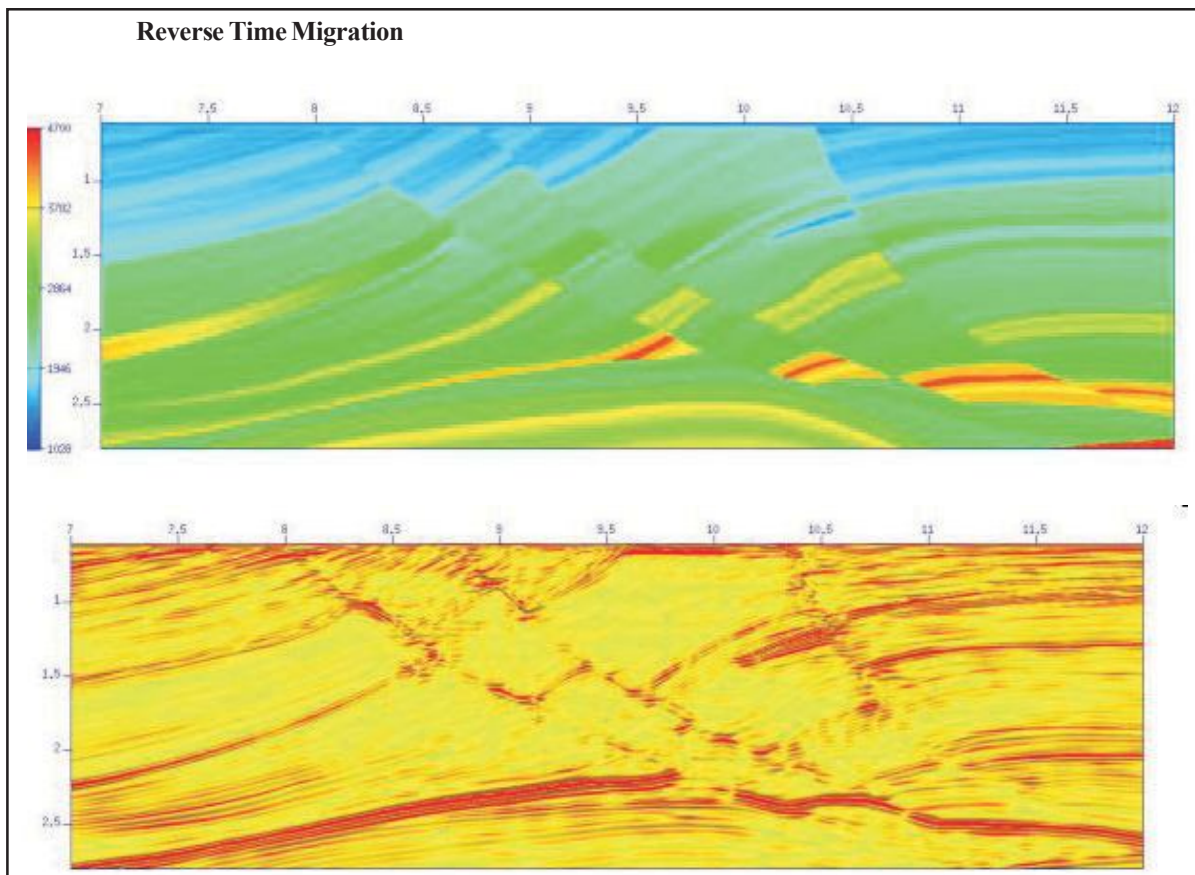


Fig.6 (a) A portion of the Marmousi2 model. (b) Reverse Time Migrated section of the synthetic data for the model shown in Figure 6a. The input data for RTM was generated using an acoustic wave propagation algorithm.

is backward propagated in time and is stored at each time step. Forward propagated wavefield and the reverse extrapolated wavefield are crosscorrelated to obtain the image. RTM can handle complex velocity models and is capable of imaging steep dips, turning waves, horizontally travelling waves, prism waves, ghosts and intrabed multiples (Jones et al., 2006).

Figure 6 illustrates the application of RTM to a part of the Marmousi2 model (Martin et al., 2006). One can observe that RTM is able to accurately image the complex geological subsurface. Now let us look at the amplitude preservation aspect of RTM.

The amplitude behaviour of RTM is studied by applying it to a very simple flat layered model shown in Figure 3. Figure 7a shows the shot gather generated by an acoustic wave modelling algorithm after muting the first arrival. One can observe the reflections from both the interfaces. The top interface has the reverse polarity whereas the bottom interface has normal polarity. This gather is used as input for RTM. The migrated offset gather is shown in Figure 7b.

Figure 8a shows the shot gather generated by an elastic wave propagation algorithm after muting first arrivals.

Besides P-P reflections from the two interfaces, one can also see P-S reflections. Next we used this data set as the input for RTM. This is precisely the case when we use real data. The real data is recorded in field after the wave propagation through a real elastic earth. The field data is then processed using algorithms based upon the acoustic wave equation. The migrated offset gather for the input of Figure 8a is shown in Figure 8b. Next let us compare the amplitude as a function of angle of incidence for the two offset gathers shown in Figures 7b and 8b against the theoretical amplitudes with the assumptions of acoustic and elastic mediums.

Figure 9 illustrates the amplitudes as a function of angle. Cyan and blue lines are the theoretical reflection coefficients under the assumption of elastic and acoustic media. Red and green lines are the amplitudes derived from the migrated offset gathers shown in Figures 7b and 8b. One can clearly observe that the amplitudes derived from migrated offset gathers follow the theoretical amplitudes computed under the assumption of acoustic medium. We are unable to recover the amplitudes of elastic medium. Therefore the assumption of acoustic wave propagation in RTM is not adequate to predict the correct amplitudes.

Amplitude preservation in RTM

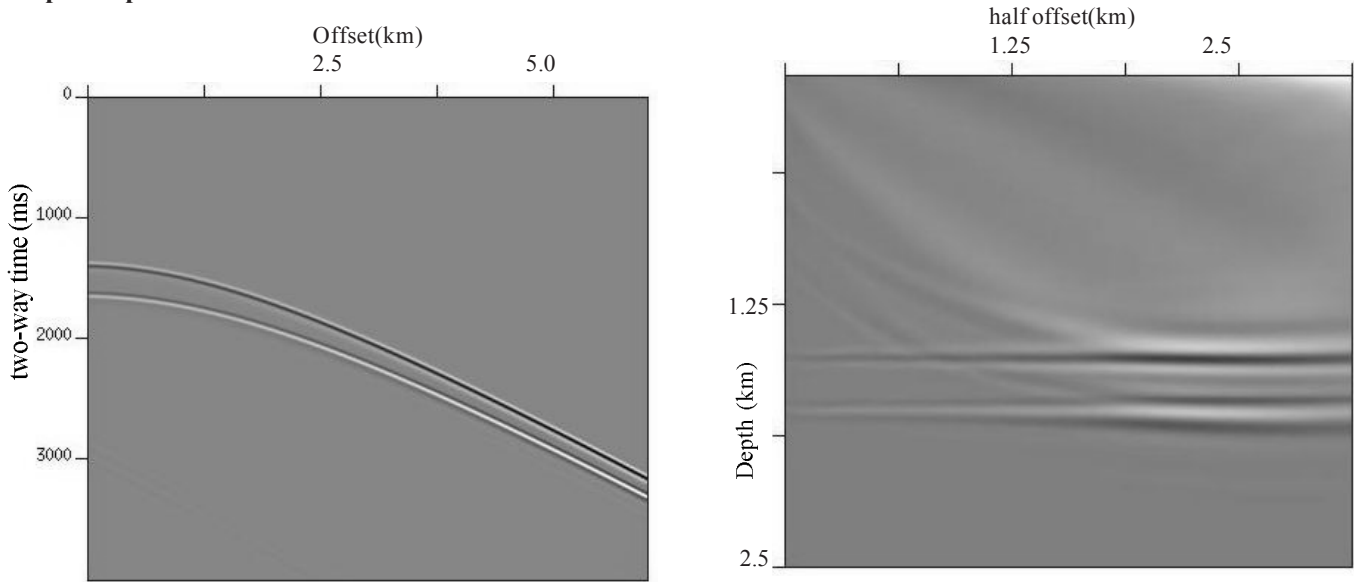


Fig.7 (a) The input gather for RTM generated using an acoustic wave propagation algorithm (b) The migrated offset gather.

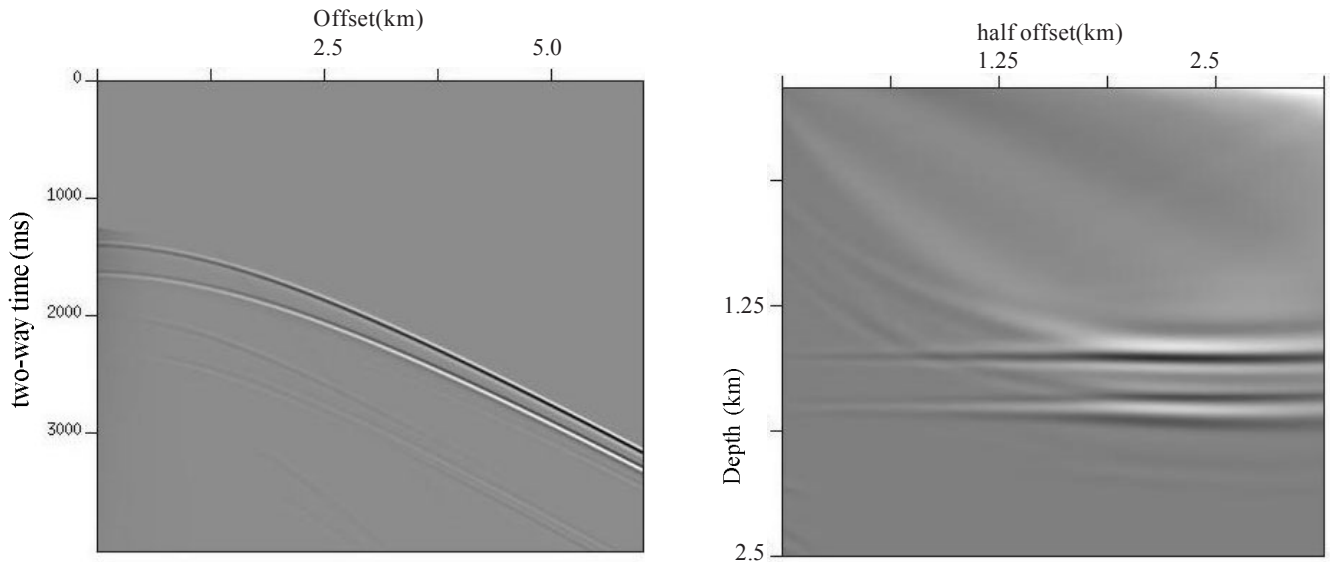


Fig.8 (a) The input gather for RTM generated using an elastic wave propagation algorithm (b) The migrated offset gather.

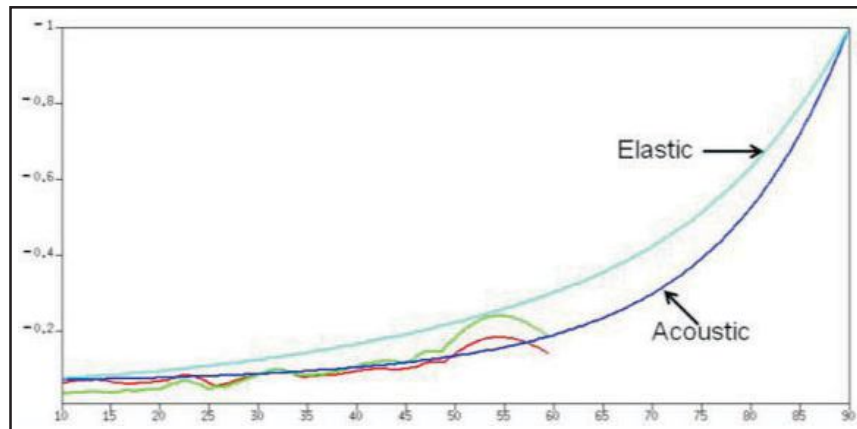


Fig.9 The reflection coefficients for the top layer in Figure 3, plotted as a function of angle of incidence. Cyan and blue lines are the theoretical reflection coefficients under the assumption of elastic and acoustic media respectively. Red and green lines are the amplitude derived from migrated gathers shown in Figures 7b and 8b respectively.

Conclusions

Today, RTM is the best available imaging algorithm in the seismic processing industry. However, amplitude preservation in RTM algorithm is dependent upon the validity of the assumption that wave propagation in the subsurface can be accurately modeled by an acoustic wave equation. In real earth, which is elastic in nature, this assumption may or may not be valid depending upon the variation in physical properties. In this paper, reflection coefficients for acoustic/elastic, acoustic/acoustic, and elastic/elastic interfaces are compared to illustrate the difference in reflection amplitudes. RTM, which uses an acoustic wave propagation algorithm, is applied to synthetic data generated by both acoustic and elastic modeling algorithms. It is shown that for a simple flat layered model the assumption of acoustic wave propagation in RTM, fails to predict the correct amplitudes. Interpreters should always bear this in mind while carrying out AVO analysis or inversion. Only for smooth velocity variations one may make the assumption of acoustic wave propagation. Prestack reverse time depth migration is usually applied to image complex geological subsurface. Therefore true amplitude processing in these situations should incorporate elastic wave propagation based algorithms.

Acknowledgements

The author would like to thank Computational research Laboratories Ltd., Pune, India, for the usage of the supercomputing system 'EKA' and the permission to publish this work.

References

Aki, K., and Richards, P. G., 1980, Quantitative seismology, W. H. Freeman and Company.

- Baysal, E., Kosloff, D. D., and Sherwood, J. W. C., 1983, Reverse Time Migration, *Geophysics*, 48, 1514-1524.
- Farmer, P. A., Jones, I. F., Zhou, H., Bloor, R. I., and Goodwin, M. C., 2006, Application of reverse time migration to complex imaging problems, *First Break*, 24, 65-73.
- Jones, I. F., Sugrue, M., King, D., Goodwin, M., Berranger, I., Zhou, H., Farmer, P., 2006, Application of reverse time migration to complex North sea imaging, *PETEX Biennial Meeting*.
- Martin, G. S., Wiley, R., and Marfurt, K. J., 2006, Marmousi2: An elastic upgrade for Marmousi, *The Leading edge*, 25, 156-166.
- McMechan, G. A., 1983, Migration by extrapolation of time dependent boundary values, *Geophysical Prospecting*, 31, 413-420.
- Virieux, J., 1986, P-SV wave propagation in heterogeneous media: velocity stress finite difference method: *Geophysics*, 51, 889-90
- Yerneni, S., D. Bhardwaj, S. Chakraborty, and S. Phadke, 2002, Finite-difference forward modeling for complex geological models, *Expanded Abstracts, Society of Exploration Geophysicists*.
- Yoon, K., Shin, C., Suh, S., Lines, L. R., and Hong, S., 2003, 3D reverse time migration using the acoustic wave equation: An experience with the SEG/EAGE data set, *The Leading Edge*, 22, 1, 38-41.